AN ABSTRACT OF THE THESIS OF

Albert Sears Crane (Name) for the Master of Science (Degree) in

Electrical Engineering (Major) presented on 12-9-70 (Date)

Title: The High Frequency Performance of a Schottky Diode Detector

Redacted for Privacy

Abstract Approved: James C. Looney

This paper analyzes the theory and performance of a Schottky barrier diode detector used over a frequency range extending from a few kilohertz into the gigahertz region. The process of large signal rectification is analyzed with the simplified detector circuit. Phenomena which can affect the rectification process at high frequencies, such as minority carrier lifetime, relaxation time, conductivity modulation and the parasitic component elements are examined. Measurements are made on each of the detector components and values derived for a network model. The model is used to predict input impedance and frequency response which is then compared to measured results.

THE HIGH FREQUENCY PERFORMANCE OF A SCHOTTKY DIODE DETECTOR

by

Albert Sears Crane

A THESIS

submitted to

Oregon State University

in partial fulfillment of
the requirements for the
degree of

Master of Science

June 1971

APPROVED:

Redacted for Privacy

Associate Professor of Electrical and Electronics Engineering
in charge of major

Redacted for Privacy

Head of Department of Electrical and Electronics Engineering

Redacted for Privacy

Dean of Graduate School

Date thesis is presented 12-9-70

Typed by Erma McClanathan for Albert Sears Crane

TABLE OF CONTENTS

I. Introduction..... 1

II. Theory of Rectification..... 3

Diode Rectification Model..... 3
Rectification Efficiency..... 9
Minority Carrier Lifetime..... 10
Conductivity Modulation..... 12
Relaxation Time..... 14
Parasitic Elements..... 15

III. Experimental Determination of Detector Elements.. 20

The Diode Detector..... 20
Diode Package and Junction Capacitance..... 22
Diode Series Resistance..... 23
Diode Series Inductance..... 26
Bypass Capacitor..... 29

IV. Composite Detector Performance..... 31

Rectification Efficiency versus Frequency... 31
Network Analyzer Measurements..... 34
ECAP Results..... 37

V. Summary and Conclusions..... 42

Bibliography..... 44

Appendix..... 46

LIST OF FIGURES

Figure		Page
1.	Basic Diode Detector Circuit.....	3
2.	Linearized Diode Model.....	4
3.	Diode Equivalent Circuit during Forward and Storage Conduction.....	5
4.	Diode Equivalent Circuit during Reverse Bias....	5
5.	Equilibrium Waveforms of the Rectifier Circuit..	7
6.	Equilibrium Values for the Rectifier Circuit....	8
7.	Effect of Series Resistance on Forward Drop.....	13
8.	Diode Equivalent Circuit.....	16
9.	Parasitic Elements of Diode Detector.....	18
10.	Ladder Equivalent of Detector.....	19
11.	Schottky Diode Detector in 50 Ohm Transmission Line Environment.....	21
12.	Junction Capacitance versus Reverse Voltage.....	24
13.	Diode Log I versus Forward Voltage.....	25
14.	Detector with Stub Line.....	27
15.	Diode Impedance with $V_r = 0$.....	28
16.	Impedance Plot of Erie Feed-through Capacitor...	30
17.	Frequency Response of Diode Detector.....	33
18.	RLC Equivalent to Give e_j/e_i.....	32
19.	Series Diode and Capacitor Impedance Using Stub Line.....	35
20.	Equivalent Input Impedance Circuit.....	36
21.	Equivalent Ladder Circuit.....	36
22.	Impedance Plot of Diode Detector.....	38

LIST OF TABLES

Table Page

1. Calculated Value for Capacitor Impedance..... 29
2. Calculated and Measured Values for Detector..... 40

THE HIGH FREQUENCY PERFORMANCE OF A SCHOTTKY DIODE DETECTOR

INTRODUCTION

High frequency, high level voltage measurements are necessary for signal generator leveling and calibration. The high frequency characteristics of a Schottky diode detector are analyzed here to better understand the problems which exist in designing a high frequency voltage detector. A flat frequency response and a constant input impedance are the primary design objectives.

Semiconductor diodes have been in use for several decades in high frequency mixing and detecting circuits. Particular attention has been given to choosing a condition which will optimize the square law detecting region for accurate microwave measurements. In recent years, however, swept frequency measurements and the desirability of calibrated and leveled generators has increased the need for precision high level detectors with low VSWR and extended frequency flatness over broad bands (7). The advent of the Schottky barrier diode with its near-ideal I-V characteristics has opened possibilities for high level voltage detection on a precision scale suitable for RF standards work. A metal-semiconductor diode was used by Ondrejka (12) at the National Bureau of Standards for peak pulse measurement. Driver and Arthur (4) have described a differential voltage

comparitor using hot carrier diodes which agree with NBS voltage standards within 2% to 1 GHz.

The diode detector as a voltage standard has several advantages over other types of RF voltage standards. For high level signals its output is two orders of magnitude greater than micropotentiometers or thermal convertors which use vacuum thermocouples. The diode is also much less susceptible to burn out due to over load. The diode itself is smaller than a thermocouple element and inherently has lower parasitic elements to affect its high frequency performance.

As with any physical device which is used for precision measurements, the parasitic elements inevitably influence electrical performance and require evaluation. This paper will evaluate the high frequency limiting mechanisms in a diode rectifier and determine the magnitude of their effects.

THEORY OF RECTIFICATION

Diode Rectification Model

The basic detector circuit is shown in Figure 1 with the diode in series between the generator and the bypass capacitor with its load resistor. The output voltage of

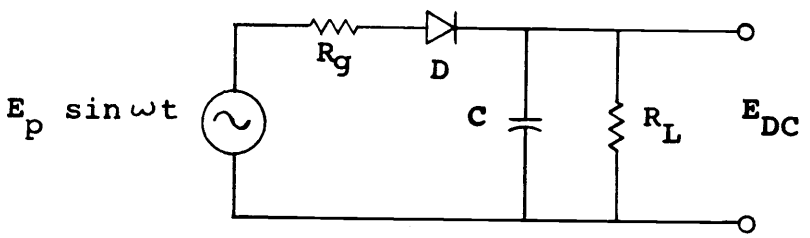

Figure 1. Basic diode detector circuit.

this low frequency model is dependent on the input voltage $E_p \sin \omega t$ and the characteristics of the diode. At low levels the output voltage is proportional to the input power level, and the detector is described as operating in the square law region. In the square law region a 1% change in input voltage will cause a 2% change in detector output voltage.

With the input voltage greater than a few tenths of a volt, the ratio of forward to reverse diode current becomes large enough that the voltage approaches a linear detection

region. A graphical solution for finding the dc output voltage and diode conduction angle based on the linearized diode model shown in Figure 2 has been developed by Krakauer (10).

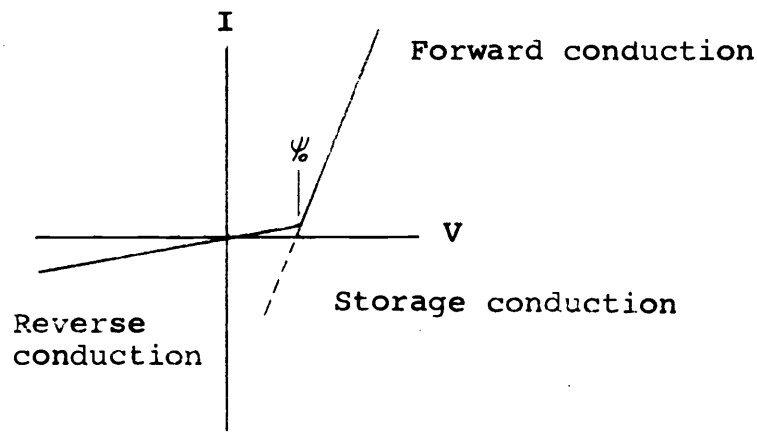

Figure 2. Linearized diode model.

The first three of the following diode parameters can be chosen to give the best fit to the diode I-V characteristics in the actual operating range.

R_f = forward resistance

R_r = reverse resistance

ψ_o = nominal electrostatic junction potential

τ = minority carrier life time. (The rate at which minority carriers spontaneously recombine to to return to thermodynamic equilibrium.)

From this model two equivalent circuits for the

detector can be drawn: one for forward conduction, Figure 3, and the other for reverse conduction, Figure 4.

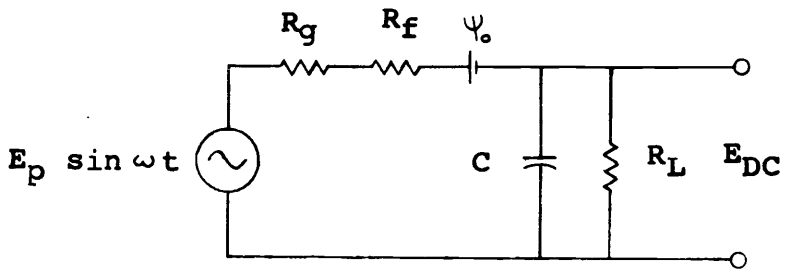

Figure 3. Diode equivalent circuit during forward and storage conduction.

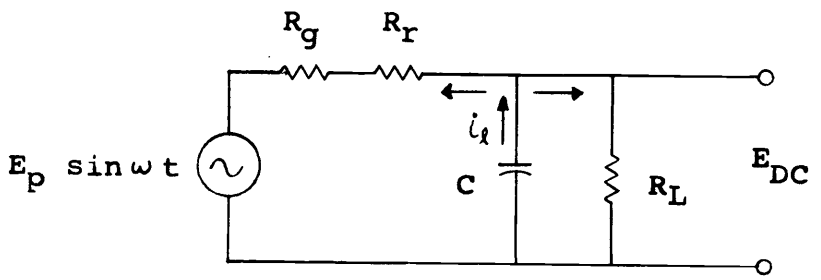

Figure 4. Diode equivalent circuit during reverse bias.

During forward conduction the effective charging resistance R_c is the combined source and diode resistance.

$$R_c = R_g + R_f \tag{1}$$

There are two currents acting to discharge C. The current through R_L is continuous and constant. The current through R_r flows when the diode is in reverse conduction and the generator emf drops below E_{DC}. Summing these two currents gives the effective leakage current, i.e.

$$i_e = \frac{E_{DC}}{R_L} + \frac{1}{2\pi} \int_{\Theta+\phi}^{2\pi+\phi} \frac{E_{DC} - E_p \sin \omega t}{R_g + R_r} d\omega t \tag{2}$$

where:

Θ = diode current initiation angle

ϕ = diode conduction angle

E_p and E_{DC} are related, Figure 5, by the sin Θ :

$$E_p = \frac{E_{DC} + \psi_o}{\sin \Theta} \doteq \frac{E_{DC}}{\sin \Theta} \tag{3}$$

Substituting and integrating yields:

$$i_e = E_{DC} \left[\frac{1}{R_L} + \frac{1 - \frac{\phi}{2\pi} + \frac{\cos \Theta - \cos (\Theta+\phi)}{2\pi}}{R_g + R_r} \right] \tag{4}$$

Since C is assumed large enough so that ripple is negligible, E_{DC} is constant and an effective discharge resistance, R_d may be calculated.

$$\frac{1}{R_d} = \frac{1}{R_L} + \frac{1 - \frac{\phi}{2\pi} + \frac{\cos \Theta - \cos (\Theta+\phi)}{2\pi}}{R_g + R_r} \tag{5}$$

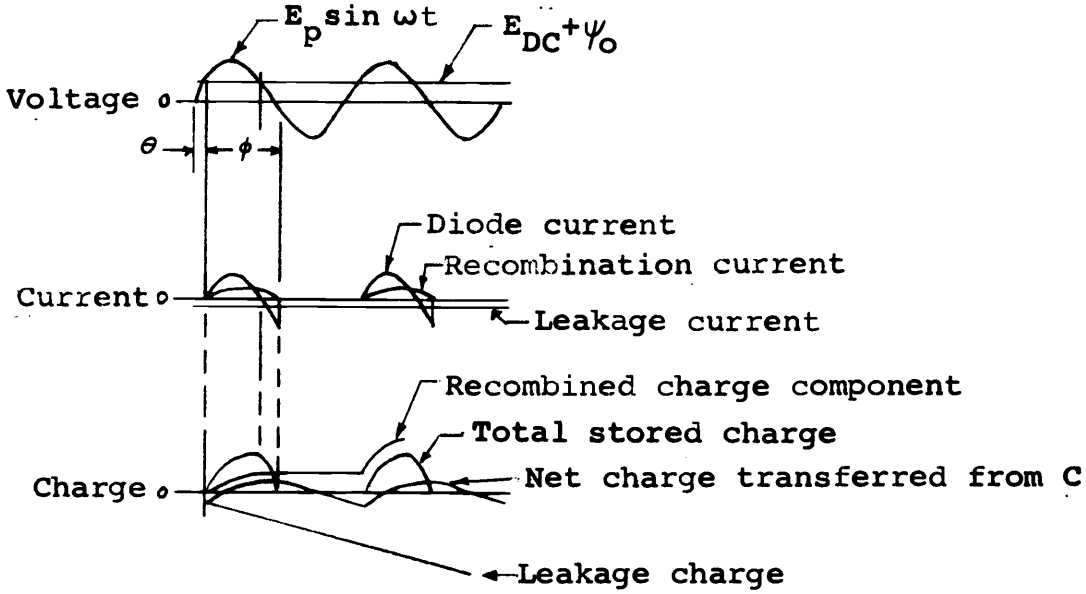

Figure 5. Equilibrium waveforms of the rectifier circuit.

The ratio of charging resistance to discharging resistance will determine the output voltage from the rectifier circuit. Combining Equations (1) and (4):

$$\frac{R_c}{R_d} = \frac{R_g + R_f}{R_L} + \frac{R_g + R_f}{R_g + R_r}\left[1 - \frac{\Phi}{2\pi} + \frac{\cos\Theta - \cos(\Theta+\Phi)}{2\pi \sin\Theta}\right] \quad (6)$$

Figure 6 shows the relationship between R_c/R_d, $\sin\Theta$, Φ and $\omega\tau$.[1] Knowing these four parameters, a value for $\sin\Theta$ can be found from the graph, and the value of E_{DC} determined from:

[1] See Appendix for equilibrium equations.

$$E_{DC} = E_p \sin \Theta - \psi_o \qquad (7)$$

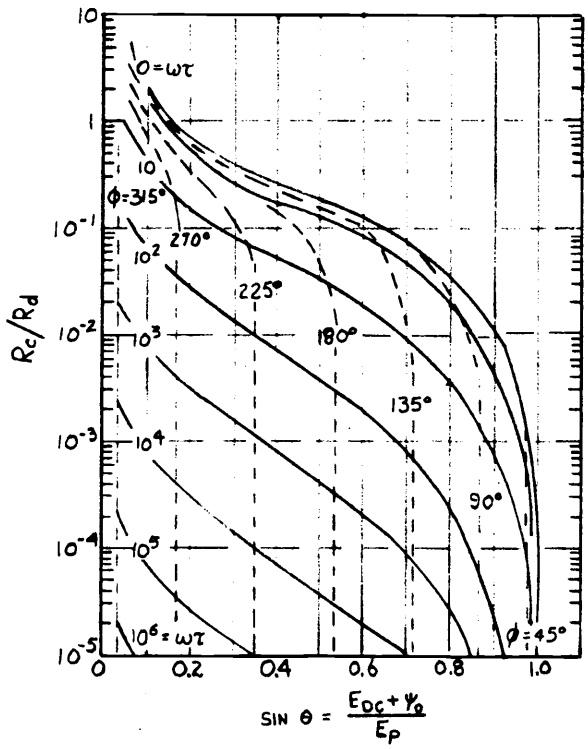

ψ_o Diode electrostatic potential
τ Diode minority carrier lifetime
R_c Effective charging resistance for C
R_d Effective discharging resistance for C
Θ Diode conduction initiation angle
Φ Diode conduction angle

Figure 6. Equilibrium values for the rectifier circuit.

Since R_c/R_d, sin Θ and Φ are not initially known, an approximation for R_c/R_d can be used to find approximate

values for sin Θ and ϕ . Letting $\Theta = 0$ in equation (6):

$$\frac{R_c}{R_d} \approx \frac{R_g + R_f}{R_L} + \frac{R_g + R_f}{R_g + R_r} \tag{8}$$

Using the approximate value of R_c/R_d, values for sin Θ and ϕ can be read from Figure 6. These values for Θ and ϕ can then be used in Equation (6) to re-evaluate R_c/R_d. With this new value for R_c/R_d Figure 3 can again be used to find more precise values for Θ and sin ϕ. Since ψ_o is given and sin Θ now determined, Equation (7) can be solved for the detector output voltage.

Rectification Efficiency

Rectification efficiency is defined as the ratio of dc output voltage to peak input voltage.

$$\text{R.E.} = \frac{E_{DC}}{E_p} = \sin \Theta - \frac{\psi_o}{E_p} \tag{9}$$

From this model analysis it is seen that the rectification efficiency is dependent on several parameters. The barrier potential ψ_o must be small compared to E_p for high rectification efficiency. Reverse leakage also will have a strong influence on the output. The ratio of forward to reverse resistance of the diode should be low. This is difficult to achieve when the peak voltage E_p is comparable to the barrier potential, since for small signals forward and back resistance approach each other.

High speed switching limitations may be present in the diode which would reduce the output at high frequencies. If minority carriers are present, there will be a stored charge in the junction. As this analysis has shown, the presence of stored charge acts as a discharge path, reducing rectification efficiency. Stored charge will become more detrimental as the time required to sweep out the stored charge becomes a larger fraction of the period. The Schottky barrier diode will now be examined to determine the extent to which stored charge and other mechanisms can limit frequency response.

Minority Carrier Lifetime

In evaluating the high frequency performance of the Schottky diode detector, a number of physical aspects of the diode exist which may place limitations on its high frequency rectification efficiency. The Schottky diode consists of a metal-semiconductor junction. In theory the conduction is by majority carriers which should be able to switch in a picosecond (2). However, actual measurements indicate additional limitations.

In a metal-n silicon diode the main conduction is by majority carriers, electrons. In forward conduction electrons are transported from the semiconductor material over the potential barrier and into the metal by thermionic energy. However, to a much lesser extent, hole flow from

the metal to the semiconductor is also present as it would be in a p-n junction. Yu (16) gives quantitative expressions for a Schottky barrier diode as follows:

$$I_{TE} = (3 \times 10^{-5} A) \left[\exp (qV_F kT) - 1\right] \text{ amperes} \qquad (10)$$

$$I_p = (3 \times 10^{-11} A) \left[\exp (qV_F/kT) - 1\right] \text{ amperes} \qquad (11)$$

where :

I_{TE} = thermionic emission current

A = diode area

q = electronic charge

V_F = forward bias

k = Boltzmann's constant

T = absolute temperature

I_p = hole current

These expressions show that the hole current is six orders of magnitude smaller than electron current, and from this standpoint can be neglected.

The presence of minority carriers will manifest itself in two particular ways. In high speed switching applications any minority carriers present in the junction must be swept out before the diode will stop conducting. Minority carriers present in the junction are referred to as stored charge. The effect of this stored charge on rectification was evaluated earlier in the rectification model. From a pulse switching point of view minority carrier life time

and switching speed are related by the diode current (8, p. 18-9):

$$t_s = \tau \ln \left(1 + \frac{I_F}{I_R}\right) \tag{12}$$

where:

t_s = switching time

τ = minority carrier life time

I_F = forward current

I_R = reverse current

Conductivity Modulation

The presence of minority carriers in a Schottky barrier diode can also be observed on the forward I-V characteristics of the diode. When the diode is conducting according to the Schottky thermionic model, current can be expressed as

$$I = I_s \left[\exp (qV/nkT) - 1\right] \tag{13}$$

where I_s is the reverse saturation current and n is the diode ideality factor which equals 1.0 for an ideal diode.

If log I is plotted versus voltage in the forward direction a straight line will be obtained. Any departure from this line will show the diode's departure from theoretical performance. At higher currents (on the order of 10 mA), the diode's ohmic resistance starts contributing with its IR drop. A departure to the right is observed as shown

in Figure 7.

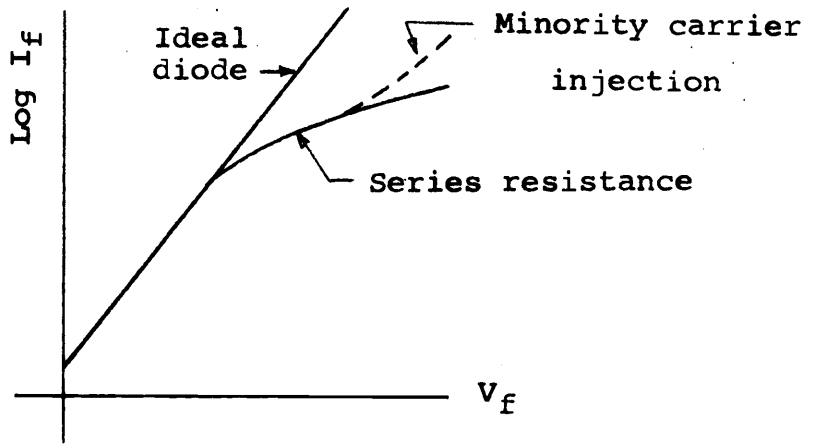

Figure 7. Effect of series resistance on forward drop.

From this graph values for R_s, the diode series resistance, can be calculated. R_s can also be observed on a linear I-V curve tracer as that portion of the curve past the knee where the trace assumes a straight line IR drop.

In an ordinary Schottky diode, as the current is increased to several tens of milliamperes it is observed that there is a decrease in the effective R_s. This is attributed to minority carrier injection which contributes to the conduction, hence the name, conductivity modulation. Lepselter and Sze (11) and Zettler and Cowley (18) have reported successful use of p-diffused guard rings at the metal edge. These reduce early reverse voltage breakdown and reverse leakage. In addition, the guard rings give

ideal emission over eight decades of forward current to 1 mA. Unfortunately, the guard rings add undesirable capacitance. Saltich and Clark (13) describe an n-p double guard ring Schottky diode which reduces some of the undesirable effects of the p-guard ring and gives substantial improvement in the forward direction. Whereas the single p-guarding showed minority carrier injection at 35 mA, the double guard ring diode showed none at the highest test current of 50 mA.

From the I-V characteristics, then, it is possible to evaluate the magnitude of minority carrier current, and the level of current at which the minority carriers and their associated stored charge will start to affect the performance of the diode as a detector. For a detector operating in the microampere range there should be no problem with stored charge.

Relaxation Time

One ultimate limiting mechanism to the Schottky barrier diode switching speed is the relaxation time of the semiconductor and the metal. The relaxation time is defined as the time constant required for a crystal lattice to return to normal equilibrium after being excited by some disturbance (1). In the case of the metal in a Schottky barrier, τ, the relaxation time, would be the time required for the "hot electron" to lose its thermal energy,

so that it can not return over the potential barrier.

The relaxation time for any crystal is given by:

$$\tau = \frac{\epsilon}{\sigma} = \epsilon\rho \qquad (14)$$

where:

ϵ = dielectric permittivity

σ = dielectric conductivity

ρ = dielectric resistivity

For a metal τ is about 10^{-17} seconds. For silicon with $\epsilon = 12(8.8 \times 10^{-12})$ F/m and = 1 ohm cm (0.01 m), τ is about 10^{-12} seconds. Hence, the semiconductor would have the slower speed of the two materials. However, 1 ps is not a severe restriction as compared to practical limitations of realizable detector circuits with their parasitic inductance and capacitance elements.

Parasitic Elements

So far, only the diode junction itself has been analyzed. Before an RF voltage wave can reach the junction, it must travel through the diode structure. The diode package is placed between the center conductor and the outer wall of a 50 ohm coaxial line. The glass package of the diode represents shunt capacitance on the diode, C_p in Figure 8. Small leads within the package have inductance, L_s. Inside the diode chip there are the ohmic contacts and the semiconductor bulk resistance, lumped together as R_s.

The barrier junction itself is a voltage variable capacitor, C_j. Figure 8, then, represents an equivalent circuit for the diode.

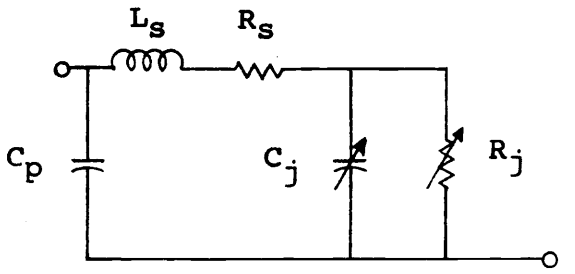

Figure 8. Diode equivalent circuit.

R_j is the voltage dependent junction resistance. For small voltage swings the dynamic resistance of R_j can be found by differentiating the diode equation (Equation 12).

$$R_j = \frac{dV}{dI} = \frac{26}{I_s} \exp\left(\frac{-V}{26}\right)$$

where:

$$\frac{nkT}{q} = 26 \text{ for ideal diode at 300 K} \qquad (15)$$

V is in millivolts

I is in amperes

Forward voltages much greater than 26 mV, this expression simplifies to:

$$R_j = \frac{26}{I} \qquad (16)$$

where:

I is in milliamperes

When the diode detector is used for rectifying signals several times larger than the barrier potential, the diode is back biased most of the cycle. On peaks the forward resistance can be determined from Equation (15). During reverse biasing on a Schottky diode, R_j will be quite high. For practical purposes it can be neglected.

The junction capacitance, C_j, is determined by the equation:

$$C_j = \frac{C_{j(0)}}{(1 - \frac{V}{V_b})^{\frac{1}{2}}} \qquad (17)$$

where:

C_j = zero voltage junction capacitance

V = junction voltage

V_b = barrier potential

For the diode detector with its peak detection circuit, the average voltage across the diode is approximately equal to the dc output voltage. Although C_j is not a constant, measurements showed that the value for C_j at the dc bias voltage could be used for predicting performance.

Perhaps the most significant parasitic element is that found in the bypass capacitor. In the detector unit shown in Figure 11, a high quality 1000 pF feed-through capacitor was used. The lead between the diode body and the capacitor

was the minimum length, about 3 mm, required by the small socket. Even this small lead inductance combined with the residual inductance of the capacitor was sufficient to give a series resonant circuit at about 100 MHz. Consequently, although the capacitor still acted as a low pass for dc current, the equivalent circuit for the capacitor over the operating range was a lossy inductor.

Figure 9 shows the high frequency equivalent circuit for the detector.

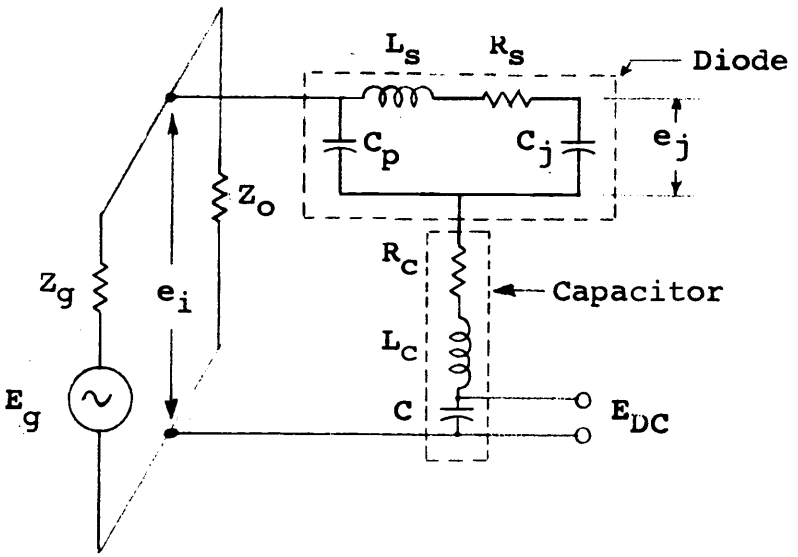

Figure 9. Parasitic elements of diode detector.

The actual RF voltage, e_j, at the junction is rectified and fed through the bypass capacitor. The reactance of C is so low above resonance that for RF analysis it can be neglected. Since R_c and L_c are common to the input circuit only, for purposes of analysis they can be

redrawn as shown in Figure 10.

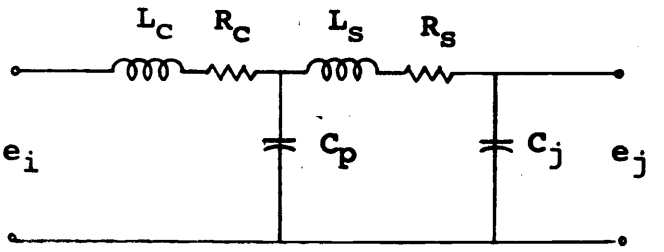

Figure 10. Ladder equivalent of detector.

EXPERIMENTAL DETERMINATION OF DETECTOR ELEMENTS

The Diode Detector

The detector configuration used in this analysis is shown in Figure 11. A 50 ohm transmission line environment was chosen to optimize the accuracy of the high frequency measurements and to reduce unwanted distributed impedance effects in the diode circuit. The transmission line is the standard 14 mm dimension with General Radio 874 connectors on each end. This size line lends itself well to the physical dimensions of a DO-7 diode package, and allows space for a diode lead socket to be embedded in the center conductor and on the bypass capacitor. The block forming the outer conductor is cut somewhat above the center line to give access to the center conductor.

This detector in the feed-through configuration permits a precision termination to be attached to the output port for impedance measurements. In addition, accurate frequency response measurements can be made by placing a power meter at the output port.

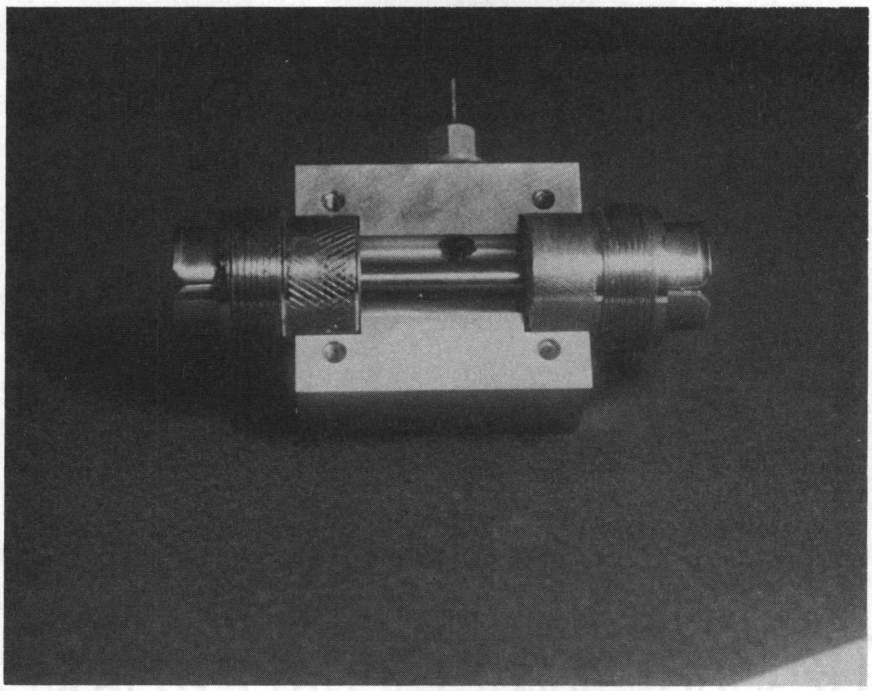

Figure 11. Schottky diode detector in 50 ohm transmission line environment.

Diode Package and Junction Capacitance

In order to determine values for C_p and C_j, the zero capacitance of the detector with the termination and the diode removed was measured on a Boonton 75D capacitance bridge. The diode was then inserted, and total capacitance versus reverse voltage measured from 0 to -15 volts. Subtracting the zero capacitance value gave total diode capacitance versus reverse voltage.

Equation (17) for junction capacitance can be rewritten in the form:

$$\frac{1}{C_j^2} = \left(\frac{1}{C_{j(0)}^2 V_b}\right) V + \frac{1}{C_{j(0)}^2} \qquad (18)$$

where:

V is positive for reverse voltage

If C_t is the total diode capacitance, and C_p the package capacitance, Equation (18) becomes:

$$\frac{1}{(C_t - C_p)^2} = \left(\frac{1}{C_{j(0)}^2 V_b}\right) V + \frac{1}{C_{j(0)}^2} \qquad (19)$$

Equation (18) is a linear equation when $1/C_j^2$ is plotted against V. Equation (19) will be a straight line only when the correct number is chosen for C_p which will make $C_j = C_t - C_p$.

Trial values were assumed for C_p and $(C_t - C_p)^{-2}$ was tabulated versus voltage from 0 to 15 volts for each trial. A linear regression was made for each line and the

correlation coefficient calculated. The best fit was obtained with C_p = 0.19 pF (correlation coefficient = 0.99995).

With the value of C_p determined, the graph, Figure 12, of junction capacitance versus reverse voltage was plotted.

Diode Series Resistance

The diode series resistance was measured from the forward I-V characteristics as shown in Figure 13. The departure from theoretical performance not only evaluates R_s, but also can indicate the presence of minority carrier injection. The average value for R_s from this graph is 7.3 ohms. For forward currents up to 70 mA, R_s appeared to be constant, indicating no minority carrier injection.

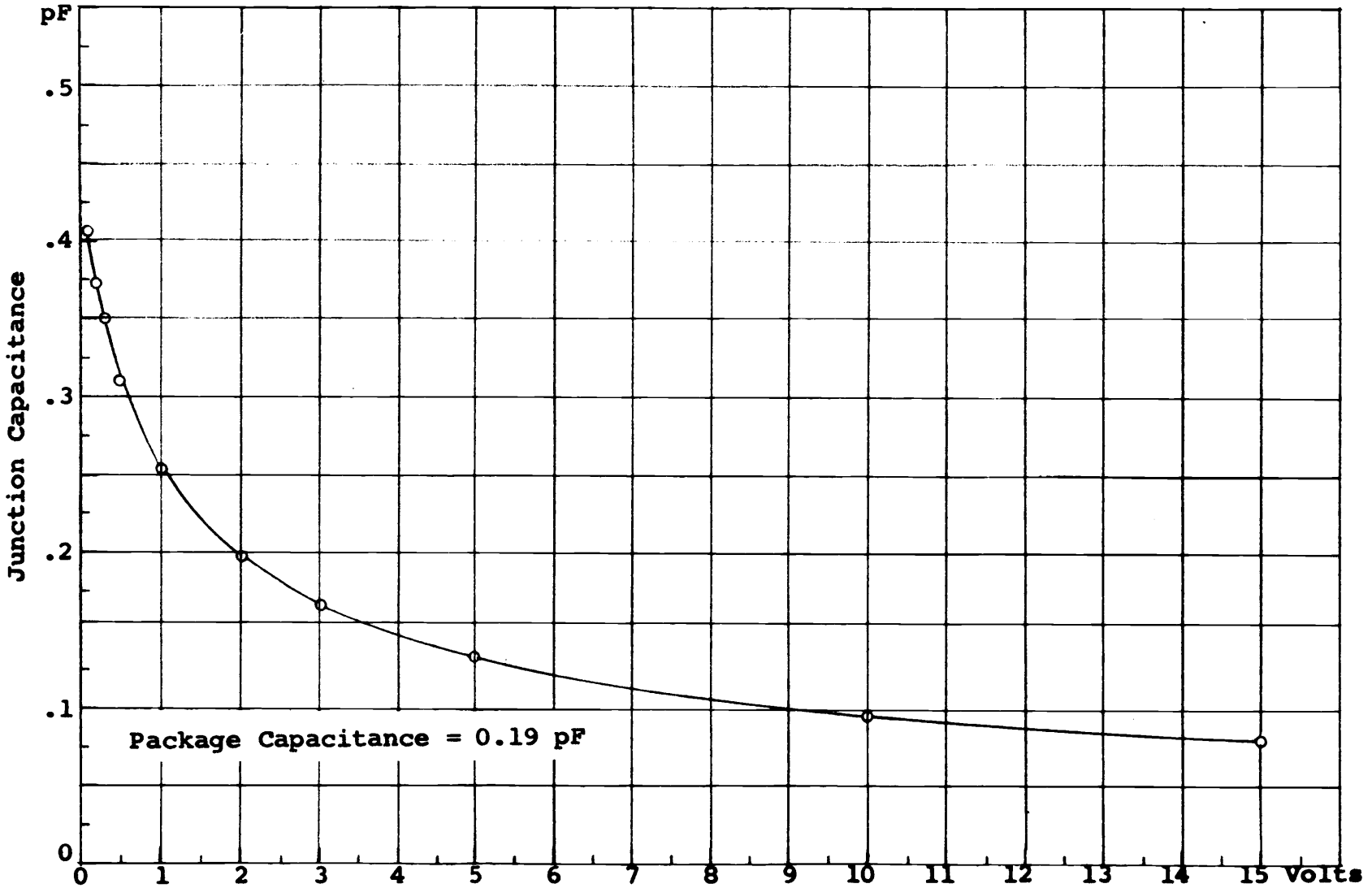

Figure 12. Junction capacitance versus reverse voltage.

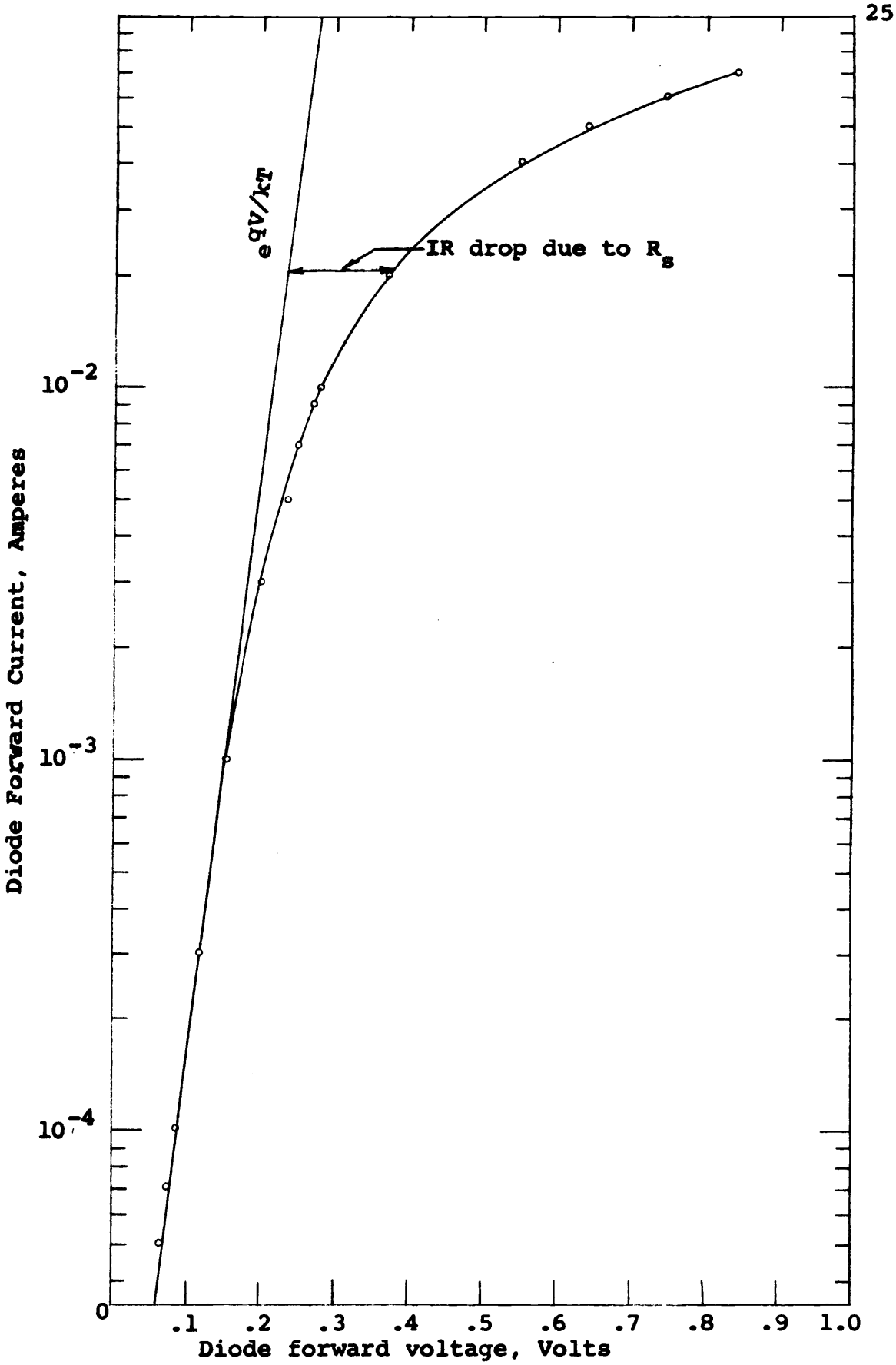
$e^{qV/kT}$
IR drop due to R_s
10^{-2}
10^{-3}
10^{-4}
0
.1
.2
.3
.4
.5
.6
.7
.8
.9
1.0
Diode Forward Current, Amperes
Diode forward voltage, Volts

Diode Series Inductance

The diode series inductance was measured using a Hewlett-Packard network analyzer. The diode was measured in the same electrical environment as it is used. A stub center conductor was made which stopped at the diode location as shown in Figure 14. This not only eliminated reflections from the end of the line, but also gave an accurate open circuit reference for the network analyzer with the diode removed.

Figure 15 is the impedance plot for the diode at zero bias from 2.0 to 4.0 GHz. The trace follows an equivalent series RLC line over the entire frequency range very well. At 2.61 GHz the series circuit is purely resistive with R_s = 6 ohms. Taking the zero capacitance value from Figure 12 as 0.435 pF, L_s calculates to be 8.6 nH.

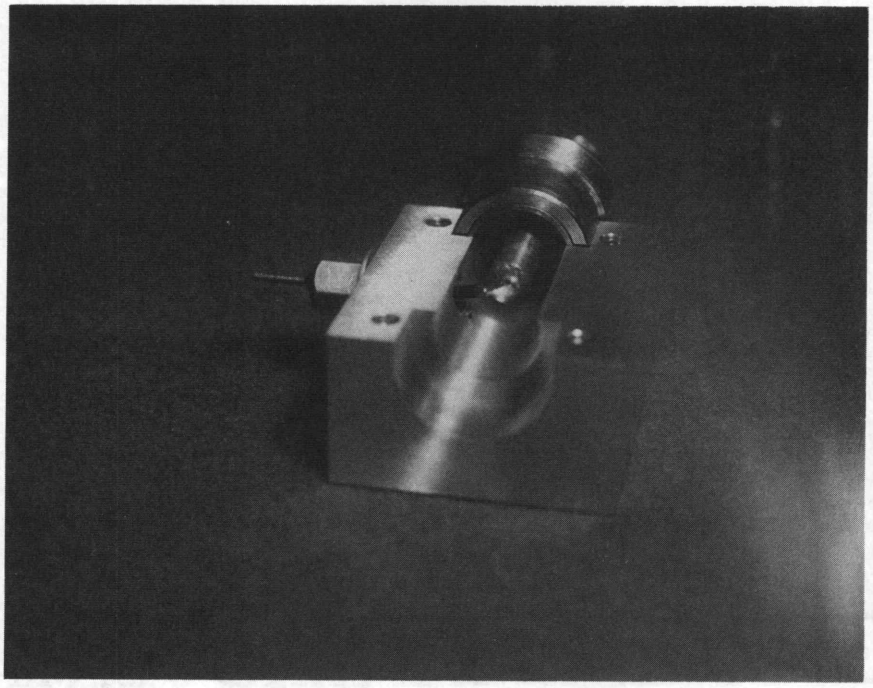

Figure 14. Detector with stub line.

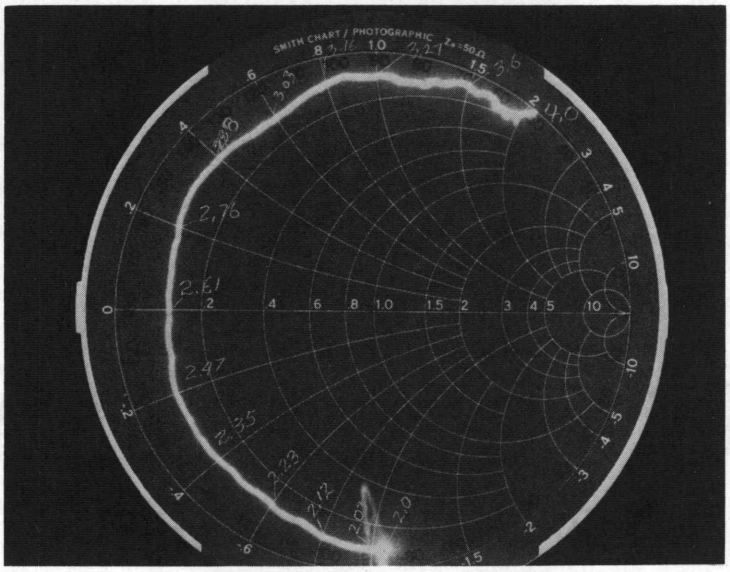

Figure 15. Diode impedance with V_r = 0. Cathode grounded, stub line, 2.0 to 4.0 GHz.

Bypass Capacitor

The electrical characteristics of the feed-through capacitor were also measured on the network analyzer. A GR-874 to female N adaptor provided a convenient plug-in fixture with which a coaxial connection to the capacitor could be made. Figure 16 a and b show the RF impedance plot of the capacitor.

Note the capacitor appears as a fairly high quality inductor up to 1.0 GHz. At 2 GHz the plot loops through a lossy resonance. Table 1 lists the values calculated for the series equivalent circuit of the impedance plots of Figure 16.

Table 1. Calculated Values for Capacitor Impedance

Frequency	X_L	L_C	R_C
0.25 GHz	3.2 ohms	2.04 nH	0
0.50	8.0	2.54	0
1.0	17.5	2.78	2
2.0	31.0	2.47	20
3.0	34.0	1.81	12
4.0	43.0	1.71	21
	Mean	2.6	

The values for R_C are not completely constant over the frequency range of interest. However, since 3.0 GHz turned out to be the maximum output for the detector, the most accurate value for this frequency was chosen, R_C = 12 ohms.

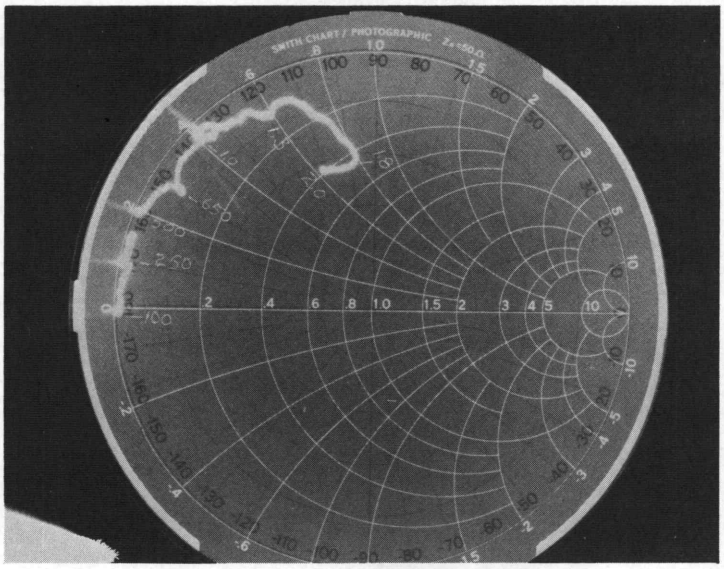

Figure 16a. Impedance plot of Erie feed-through capacitor. 0.1 to 2.0 GHz.

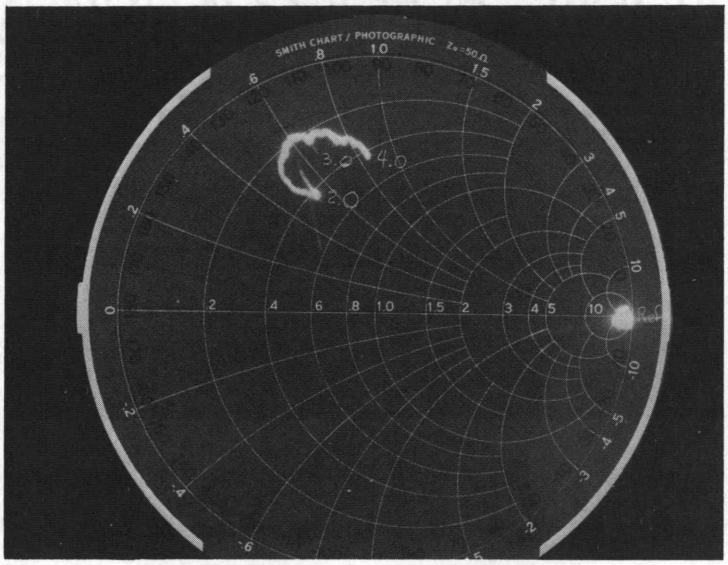

Figure 16b. Impedance plot of Erie feed-through capacitor. 2.0 to 4.0 GHz.

COMPOSITE DETECTOR PERFORMANCE

Rectification Efficiency versus Frequency

One of the primary objectives for examining the mechanisms involved in the diode detector is to be able to develop a model that will predict the rectification efficiency versus frequency. Often it is more important to know relative frequency response than the actual value for rectification efficiency. After an accurate low frequency ac voltage measurement has been made, this voltage level can be extended to high frequencies with the detector of known frequency response.

In order to accurately evaluate the model, it was necessary to make a high frequency response measurement on the detector. The output of the detector was fed through a 6 db attenuator to an HP 431C power meter. Originally the input level to the power meter was held constant at a power equivalent to 1.0 volt peak on the transmission line. The disadvantage of having a constant incident voltage response is that the changing dc output voltage affects the junction capacitance, and the equivalent circuit is not constant.

By holding E_{DC} = 1.0 V constant for the entire frequency range, the variation in C_j is avoided. The incident voltage on the detector is allowed to vary and the equivalent response from the power meter reading is calculated from the relationship:

$$\frac{V_1}{V_2} = \sqrt{\frac{P_1}{P_2}} \tag{20}$$

Figure 17 shows the results of these frequency response measurements. The predominant landmark on the curve is the nearly six times increase in output voltage at 2.8 GHz. One wonders if this is simply a series resonant RLC with $Q = E_{DC}/e_i = 5.7$.

If a value for $C_{j(0)} = 0.255$ pF is used to find R and L from $Q = X_c/R$ and $L = 1/\omega^2 C$, the values in Figure 18 are obtained.

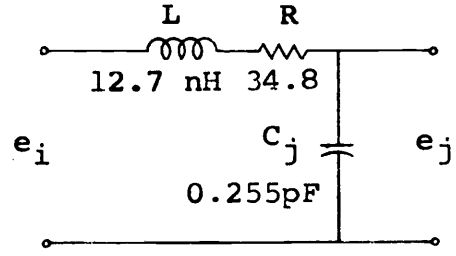

Figure 18. RLC equivalent to give e_j/e_i.

The voltage transfer function for this circuit is:

$$\frac{e_j}{e_i} = \left[1 + \left(\frac{\omega}{\omega_o}\right)^2 \left(\frac{1}{Q^2} - 2\right) + \left(\frac{\omega}{\omega_o}\right)^4\right]^{-\frac{1}{2}} \tag{21}$$

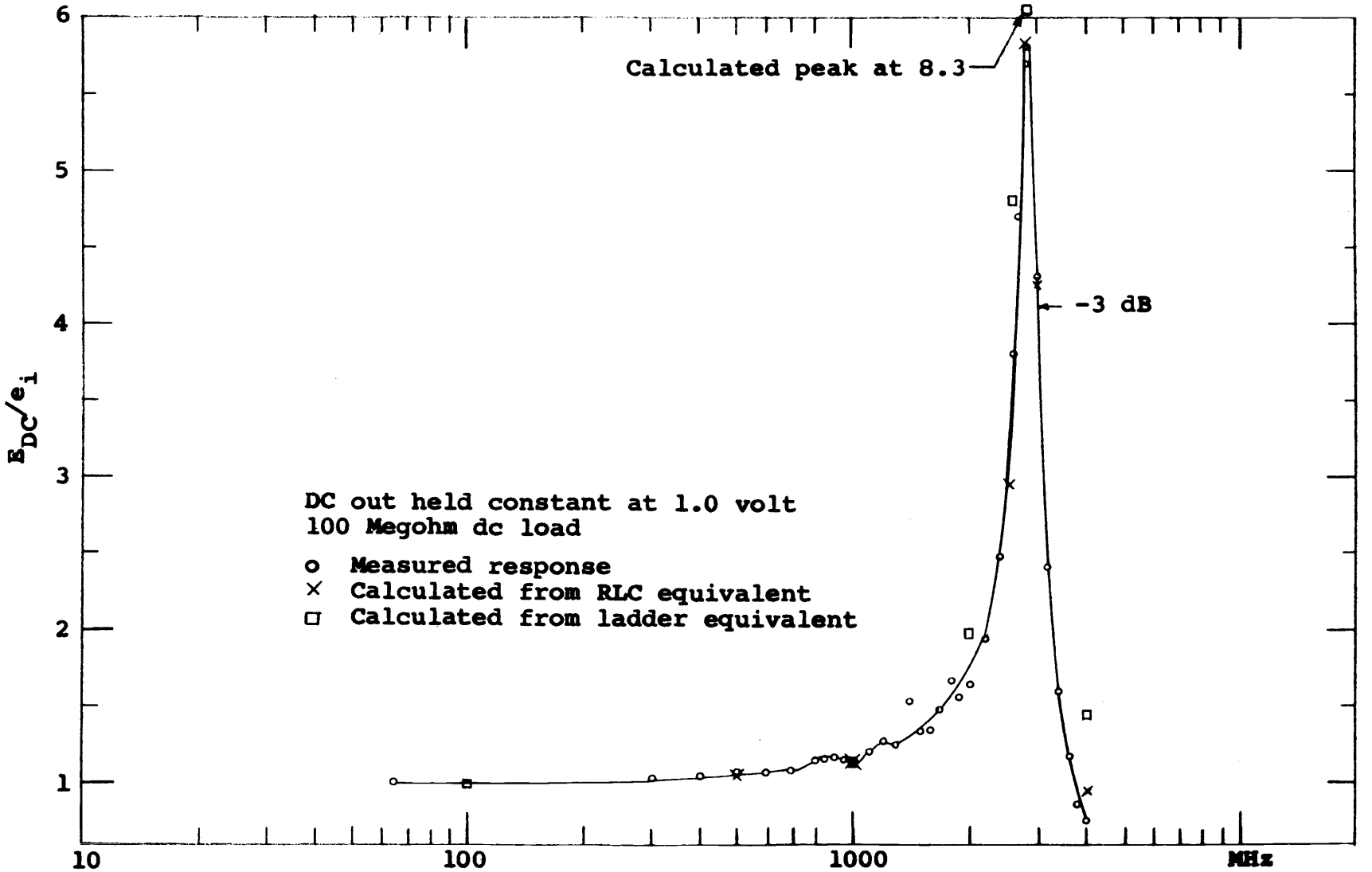

Figure 17. Frequency response of diode detector.

Several points were calculated from this equation and plotted on the measured response as an "X" in Figure 17. These points fit the curve very well over the whole range. Note, however, that the actual frequency response measurements show some aberrations between 1 and 2 GHz. These were probably caused by imperfections in the bypass capacitor which were observed also in Figure 16.

Having examined the voltage transfer model, the impedance measurements will now be analyzed to see if they agree with this model.

Network Analyzer Measurements

If frequency response is the only result desired, Figure 18 is a good model. It does not tell the whole story, however. First, the 3db points in Figure 17 give an equivalent Q of 7.4. This indicates a higher order function. Also, the input impedance for the detector calculated from this model does not agree well with measurements.

Figure 19 shows the impedance plot of the diode in series with the bypass capacitor. Figure 20 is an equivalent circuit for this combined impedance which fits very well over the 2 to 3 GHz range.

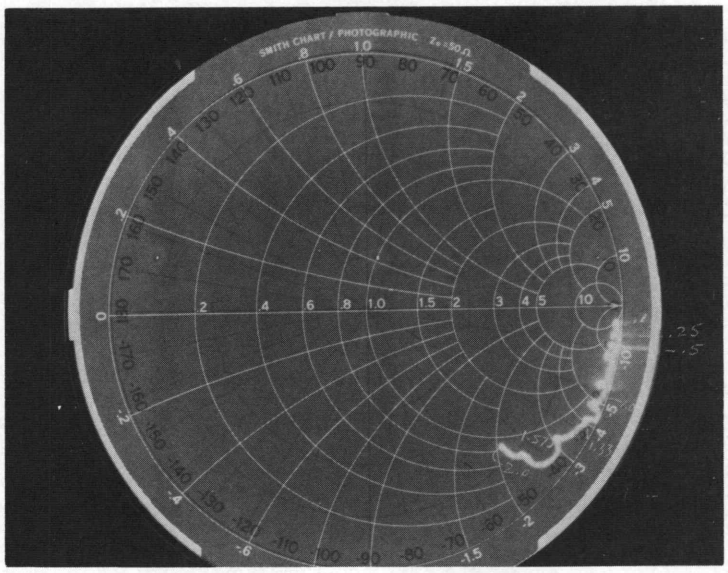

Figure 19a. Series diode and capacitor impedance using stub line. V_r = 0, 0.1 to 2.0 GHz.

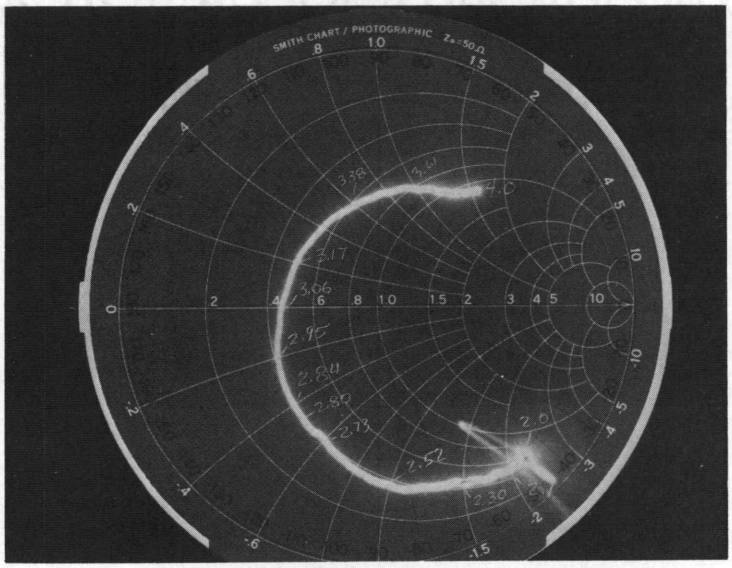

Figure 19b. Same as above, 2.0 to 4.0 GHz.

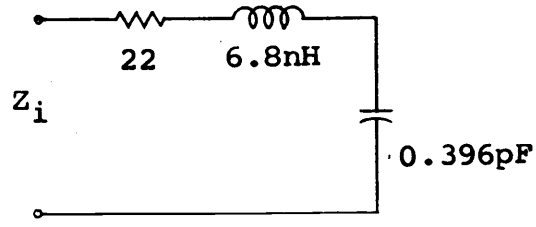

Figure 20. Equivalent input impedance circuit.

Note that the impedance equivalent circuit is not the same as the e_j/e_i circuit of Figure 18.

A complete model which can predict both impedance and rectification efficiency flatness is the ladder network of Figure 10. Figure 21 is this circuit with the various elements shown as measured.

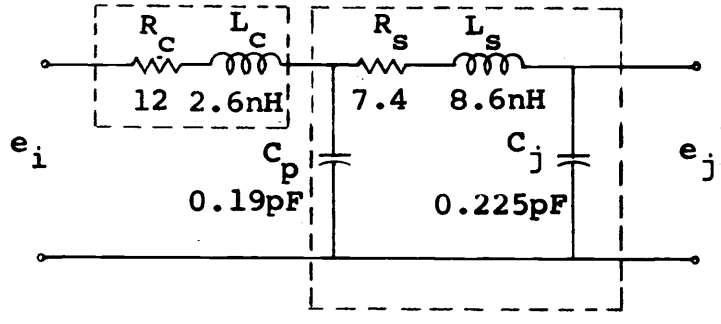

Figure 21. Equivalent ladder circuit.

Figure 22 shows the network analyzer[2] plot of the detector terminated in 50 ohms. The impedance values shown in Figure 19, when paralleled with 50 ohms, yield the values measured in Figure 22.

ECAP Results

To check the validity of the composite model, a Tymshare computer program for AC analysis was run on the circuit of Figure 21. The results of this analysis are shown in Table 2 in a comparison with measured data. The calculated values for e_j/e_i are shown as " □" points on the curve in Figure 17.

[2]Impedance measurements of the detector were made with the network analyzer which has an incident signal in the neighborhood of 50 mv. External bias was used to set E_{DC} = 1.0V. To verify that this was equivalent to the input impedance with self bias equal to one volt, a slotted line measurement was made with e_i = 1 volt. The two measurements, taken at 1 GHz, agreed within 5% of each other, well within system error limits.

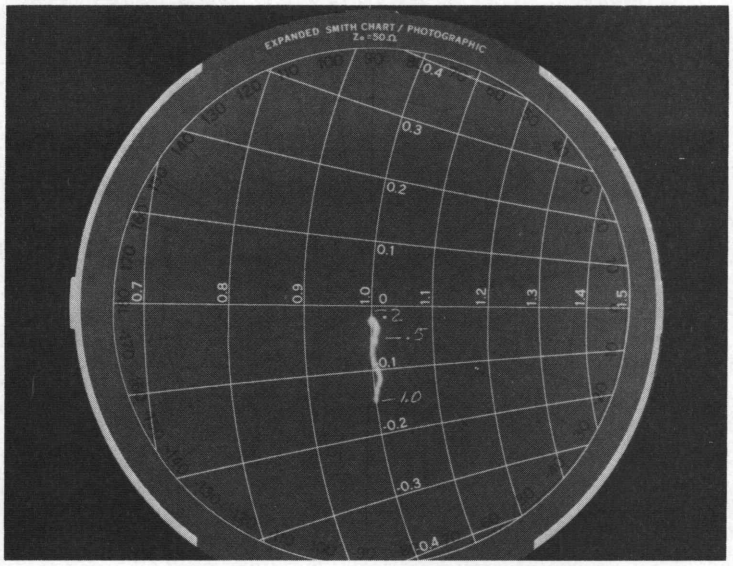

Figure 22a. Impedance plot of diode detector. 1.0 volt bias, 0.2 to 1.0 GHz.

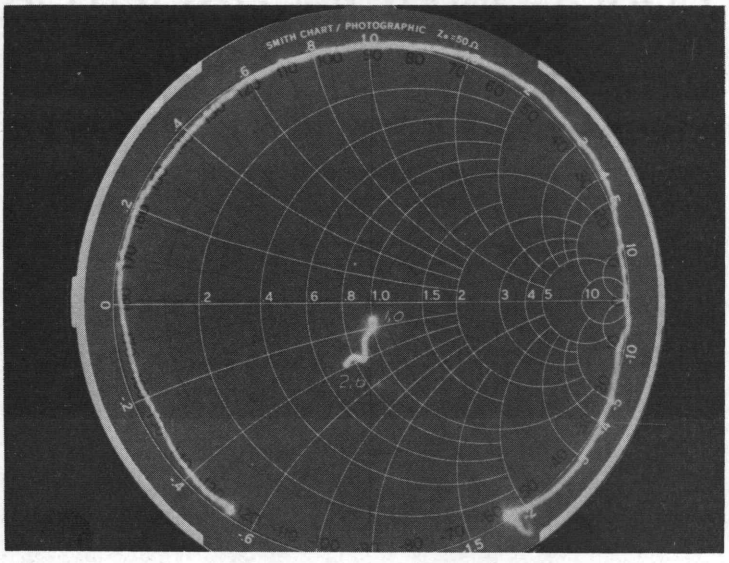

Figure 22b. Same as above, 1.0 to 2.0 GHz.

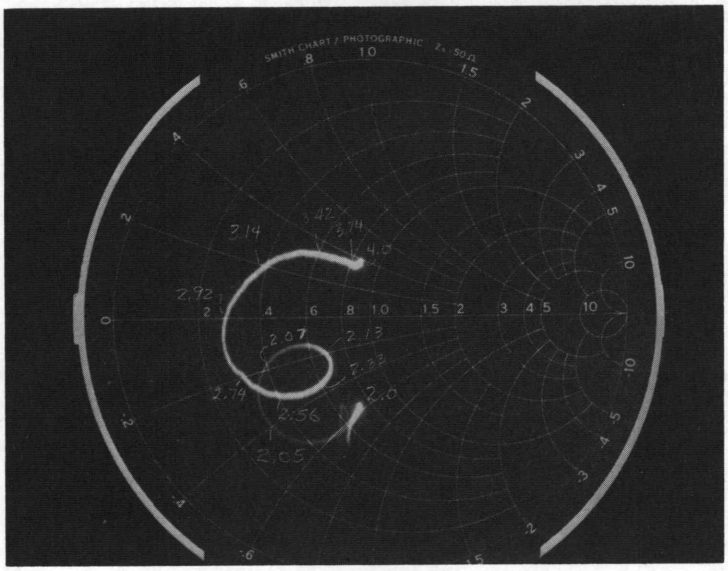

Figure 22c. Impedance plot of diode detector. 1.0 volt bias, 2.0 to 4.0 GHz.

Table 2. Calculated and Measured Values for Detector

Freq.	e_j/e_i		Normalized Input Impedance	
GHz	ECAP	Measured	ECAP	Measured
0.1	1.001	1.00	1.000 -j0.014	1.0 -j0.01
1.0	1.148	1.16	0.970 -j0.149	1.0 -j0.15
2.0	1.982	1.64	0.784 -j0.340	0.75-j0.38
2.6	4.806	3.80	0.409 -j0.294	0.35-j0.30
2.8	8.107	5.70	0.293 -j0.126	0.28-j0.15
3.0	8.304	4.31	0.292 -j0.095	0.30-j0.08
4.0	1.440	0.74	0.858 -j0.259	0.85-j0.38

The calculated and measured values for e_j/e_i in Table 2 show good agreement for predicting the resonant frequency for the network. The computed output voltage is generally higher than the measured value. The ECAP program predicted a peak of 8.3 whereas 5.7 was the maximum measured. This could be due to some error in the measurement of R_s which made the diode look less lossy than it actually was. One wonders if perhaps there is some stored charge reducing the rectification efficiency slightly. This seems unlikely since it was not observed at all on forward I-V measurements.

Comparing calculated input impedance with measured values shows agreement to about the accuracy limit of the network analyzer. At 100 MHz both methods give Z_i = 50 ohms with about 1% capacitive reactance. At 1.0 GHz

the reactance is up to about 15%, but resistance is still within 1%. Both real and imaginary parts have close agreement up to 4 GHz. Note that ECAP yielded a purely resistive input between 2.8 and 3.0 GHz. The analyzer measured zero phase shift at 2.92 GHz.

SUMMARY AND CONCLUSIONS

This paper has examined the rectification process involved in a detector using a Schottky barrier diode. Since stored charge is essentially negligible in a Schottky diode, the height of the barrier potential is the most significant parameter in determining rectification efficiency.

It was shown that the presence of minority carriers, which would degrade the high frequency performance, can be observed on the logarithmic I-V plot of the DC forward characteristics of the diode. The TI Schottky diode used in the experiment did not show evidence of conductivity modulation even at a forward current of 70 mA. Relaxation time for the silicon crystal in the Schottky diode is on the order of 10^{-12} seconds. This represents an insignificant limitation when operating in the gigahertz frequency range.

Of all the high frequency limitations discussed here, it is obvious that the parasitic elements play the largest role in limiting frequency response. The equivalent circuit for the detector was shown to be a two-section LRC ladder which had a peak resonance output at 2.8 GHz. The lead inductance of the diode and the internal inductance of the bypass capacitor are primarily responsible for this peaking.

If improvements are to be made, it should be in

reducing these parasitic effects. The package capacitance could be designed into the transmission line, and diode packages with lower inductance are available. Finally, the bypass capacitor should have as little inductance as possible. However, capacitors with sufficient size for the low frequency range are likely to have inductance when used at microwave frequencies.

By using the equivalent circuit developed with the methods presented here, it is possible to predict the frequency response of a precision detector. Design improvements then can be made to the detector or corrections calculated for its response.

BIBLIOGRAPHY

1. Alder, R. B., A. C. Smith and R. L. Longini. Introduction to semiconductor physics. New York, John Wiley, 1964. 247p.

2. Cowley, A. M. and H. O. Sorensen. Quantitative comparison of solid state microwave detectors. IEEE Transaction on Microwave Theory and Techniques MTT-14 (12):588-602. 1966

3. Cowley, A. M. Titanium-silicon Schottky barrier diodes. Solid State Electronics 12:403-414. 1970

4. Driver, L. D. and M. Gerald Arthur. A wideband RF voltmeter comparator. I.R.E. Transactions on Instrumentation and Measurement IM-17 (Z):146-150. 1968

5. Gray, Paul E. et al. Physical electronics and circuit models of transistors. New York, John Wiley, 1964. 262p.

6. Hewlett-Packard. The hot carrier diode theory, design and application. Application note 907. Palo Alto, California. 15p.

7. Hosking, M. W. Coaxial wide band detector type 6060. Marconi Instrumentation 12 (3):45-48. 1969

8. Hunter, Lloyd P. Handbook of semiconductor electronics. 3d ed. New York, McGraw-Hill, 1970. 21 Sections.

9. Krakauer, Stewart M. and S. W. Soshea. Hot carrier diodes switch in picoseconds. Electronics 36:53-55. July 19, 1963.

10. Krakauer, Stewart M. Harmonic generation, rectification, and lifetime evaluation with step recovery diode. Proceedings of the I.R.E. 50 (7):1665-1676. 1962

11. Lepselter, M. P. and S. M. Sze. Silicon Schottky barrier diode with near-ideal I-V characteristics. The Bell System Technical Journal 47 (2):195-208. 1968

12. Oudrejka, A. R. and P. A. Hudson. Measurement standards for low and medium peak pulse voltages. Journal of Research of National Bureau of Standards 70C (1):13-18. 1966

13. Saltich, J. L. and L. E. Clark. Use of a double diffused guard ring to obtain near ideal I-V characteristics in Schottky barrier diodes. Solid State Electronics 13:857-863. 1970

14. Shive, John N. The properties and physics of semiconductor devices. Princeton, Van Nostrand, 1959. 487p.

15. Sorenson, Hans O. Using the hot carrier diode as a detector. Hewlett-Packard Journal 17 (4):2-5. 1965

16. Yu, A. Y. C. The metal-semiconductor contact: an old device with a new future. IEEE Spectrum 7 (3):83-89. March 1970

17. Yu, A. Y. C. and E. H. Snow. Minority carrier injection of metal-silicon contacts. Solid State Electronics 12:155-160. 1969

18. Zettler, R. A. and A. M. Cowley. P-n junction - Schottky barrier diode. IEEE Transactions on Electron Devices Ed-16 (1):58-63. 1969

APPENDIX

APPENDIX

Steady-state Equilibrium Equations for Rectifier

Continuity of stored charge for steady-state equilibrium (1) is:

$$\frac{dQ}{dt} + \frac{Q}{\tau} = i_d$$

where:

$$i_d = \text{diode current}$$

$$= \frac{E_p}{R_c} \sin (\omega_1 t + \Theta - \sin \Theta)$$

$$\Theta = \sin^{-1} \left[\frac{E_{DC} + \psi_o}{E_p} \right]$$

Solution to charge equation:

$$Q = \left[\frac{E_p \sin \Theta}{R_c} \right] \left[\frac{\omega_1}{\omega_1^2 + \tau^{-2}} \right] \left[\left(\frac{\cot \Theta}{\omega_1 \tau} + 1 \right) \sin \omega_1 t + \left(\frac{1}{\omega_1 \tau} - \cot \Theta \right) \cos \omega_1 t + (\cot \Theta + \omega_1 \tau) \epsilon^{-\omega_1 t / \omega_1 \tau} - \left(\frac{1}{\omega_1 \tau} + \omega_1 \tau \right) \right]$$

Equilibrium conditions:

1. $Q = 0$ at $\omega_1 \tau = \Theta + \phi$
2. Capacitor added charge per cycle = diode recombination charge = charge lost through R_L

Parameter relationships:

$$\cot \Theta = - \frac{\omega_1\tau \sin \phi - \cos \phi + \omega_1{}^2\tau^2(1-\epsilon^{-\phi/\omega_1\tau}) + 1}{\sin \phi - \omega_1\tau \cos \phi + \omega_1\tau\, \epsilon^{-\phi/\omega_1\tau}}$$

$$\frac{R_c}{R_d} = \frac{1}{2\Pi}\left(\frac{\omega_1\tau}{\omega_1{}^2\tau^2+1}\right)\left[\left(\frac{\cot \Theta+1}{\omega_1\tau}\right)(1-\cos \Theta) + \left(\frac{1}{\omega_1\tau} - \cot \Theta\right)\sin \phi + \right.$$

$$\left. \omega_1\tau\ (\cot \Theta + \omega_1\tau)\ (1 - \epsilon^{-\phi/\omega_1\tau}) - \phi\ (\frac{1}{\omega_1\tau} + \omega_1\tau)\right]$$